

Auto-Calibrated Dynamic Parallel MRI with Phase-Sensitive Data

Jong Bum Son and Jim X. Ji

Department of Electrical and Computer Engineering, Texas A&M University

Abstract—A number of MRI applications rely on dynamic phase information embedded in the acquired images. Such applications often require multiple acquisitions, leading to possibly long scan time and low temporal resolution. Previously, SENSE method has been used for phase-sensitive data to shorten acquisition time. However, SENSE can be subject to artifacts due to inaccurate coil sensitivities and low SNR. In this paper, dynamic phase data are derived from self-calibrated parallel MRI and an optimal method is used to combine phase information from multiple receiver channels. Simulation results using 4-channel prostate imaging data show that it is possible to get a factor of 3 speedup and the new method is more accurate than the SENSE method in reconstructing the phase information, thus has potential to improve phase-sensitive MRI applications such as phase contrast velocity mapping, temperature mapping for thermal therapy, and Dixon water/fat imaging.

Keywords—Parallel MRI, phase sensitive MRI, phase-contrast MRA, temperature mapping, image reconstruction

I. INTRODUCTION

A number of important MRI applications rely on image phase to provide critical information. A partial list includes proton resonance-based MR temperature mapping, phase-contrast velocity mapping for flow imaging in MR angiography, Dixon water/fat imaging, and phase-sensitive inversion recovery MRI [1-5]. In these applications, a key disadvantage is the long scan duration to acquire the imaging data. To detect the useful phase information, they require at least two acquisitions to estimate and remove the background phase caused by B_0 field inhomogeneity and other factors such as eddy currents. In addition, multi-slice acquisitions are often needed to obtain 3-dimensional (3D) information (e.g. 3D flow velocity or temperature maps), leading to significantly longer acquisition time. Perhaps more importantly, slow data acquisition could severely limit the utility of MRI phase imaging in certain applications where high temporal resolution is needed such as temperature monitoring in thermal therapy.

With the technical advance in parallel MRI (pMRI) using phase-array coils and multiple-channel receivers, significant scan time reduction is possible, which can benefit the aforementioned phase-sensitive MRI applications [6]. In particular, it has been shown that when a reference scan is available and the object is stationary, SENSE (Sensitivity Encoding) with the reduction factor of two ($R = 2$) is rather

accurate in tracking the dynamic temperature change using phase information during thermal ablation [3]. For water/fat imaging, one- or multi-point Dixon techniques have been successfully combined with SENSE to improve scan-efficiency [7,8]. A potential problem in using SENSE is that it requires highly accurate coil sensitivity, which can be difficult to estimate in practice. In addition, low SNR and artifacts due to sensitivity error limit the reduction factors to be low [9,10].

Self-calibration pMRI techniques such as auto-SMASH (Simultaneous Acquisition of Spatial Harmonics), GRAPPA (Generalized Autocalibrating Partially Parallel Acquisition), PARS (Parallel MRI with Adaptive Radius in k-space), and MCMLI (Multi-Column Multi-Line Interpolation) can overcome or alleviate the problem by collecting calibrating data together with the imaging data [11-16]. However, these methods are usually optimized for high signal-to-noise ratio (SNR) of the magnitude image, but not for that of the phase image. For example, the sum-of-squares (SOS) reconstruction used to obtain the magnitude image in fact eliminates the phase information altogether.

In this paper, phase sensitive imaging data are derived from self-calibrated k-space reconstructions. An optimal method to combine phase information from multiple channels is used. The method is based on a least-square criterion to obtain high-SNR phase information. In addition, the phase wrapping problem in phase subtraction is automatically handled using complex vectors. Simulation results using 4-channel prostate imaging data show that the new method is more accurate than the SENSE method in recovering the phase information and it is robust against the image noises even in the low sensitivity areas of particular receiver coils.

II. METHODOLOGY

In this section, we describe the auto-calibrated image reconstruction method and an optimal method to combine multiple-channel images in pMRI with phase-sensitive data.

Adaptively Auto-Calibrated pMRI Reconstruction

Autocalibration techniques such as Auto-SMASH [11,16] and GRAPPA [12] have the potential to provide improved reconstruction, partially because they use dynamically acquired calibration data and avoid the need for pre-determined coil sensitivity. As a result, they are more robust to motion, reduce the aliasing artifacts, and improve the SNR. For example, in GRAPPA, a few additional auto calibration signal (ACS) lines are collected in the central k-space without subsampling, which are used to train a linear interpolation model. Then, the model is used to interpolate

the missing k-space data from sampled data sets in a coil-by-coil fashion. An illustration of the interpolation net and ACS lines is shown in the Fig. 1 (a). MCMLI is an improved GRAPPA method that uses an expanded 3D linear interpolation model including coils, neighboring blocks (k_y), and adjacent frequency encoding columns (k_x) as input. In addition, it utilizes a floating-net fitting method that treats all available central lines as ACS [13], which increases the number of training equations and numerical stability.

Once the unknown coefficients were determined, missing k-space lines are interpolated, followed by 2D inverse FT to obtain coil images. In conventional imaging, these images will be combined using sum-of-squares (SOS) to obtain a high SNR magnitude image. For phase imaging as discussed here, this is not desirable as SOS loses all phase information.

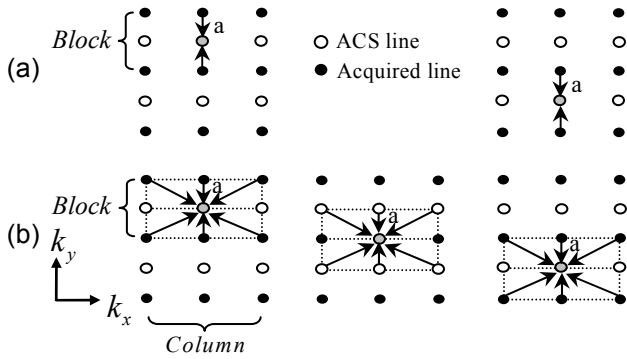


Figure 1. Illustration of interpolation models and coefficient fitting schemes of (a) GRAPPA and (b) MCMLI. MCMLI uses an interpolation net including both neighboring phase encoding and frequency encoding lines from multiple channels (not shown) as inputs. Full k-space data sets are interpolated using the model, once the interpolation coefficients are determined.

Optimal Phase Information Combination from Multi-channel Data

In dynamic imaging, a sequence of image frames are acquired using L channels. The reconstructed complex image for the c^{th} channel and t^{th} frame can be written as

$$I_c^t(x, y) = |S_c(x, y)I'(x, y)| e^{j\theta_c(x, y)} e^{j\Delta\theta^t(x, y)} \quad [1]$$

where $S_c(x, y)$ is the coil sensitivity, $\theta_c(x, y)$ represents the spatially varying phase factor due to wavelength effect and electronic delay, and $\Delta\theta^t(x, y)$ is the phase difference introduced by the subject (e.g. due to the change of temperature or velocity). This dynamic phase difference is of our interest in most applications.

An intuitive method to extract $\Delta\theta^t$ is simply averaging the phase images over all channels. However, this is not desirable because: (1) the coil-dependent phase factor $\theta_c(x, y)$ could lead to phase cancellation; and (b) coil images have space-varying SNR because of localized coil

sensitivities. Even if $\theta_c(x, y)$ can be removed, averaging is not optimal in terms of SNR of the phase information. To overcome these two problems, the phase difference map is extracted and combined using

$$\Delta\theta^t(x, y) = \arg \sum_{c=1}^L (I_c^t(x, y) \cdot I_c^{\text{ref}}(x, y)^*) / \sigma_c^2 \quad [2]$$

where $I_c^{\text{ref}}(x, y)$ is a complex reference image (normally selected to be the first frame) and σ_c^2 is the noise power of the c^{th} channel (assuming noise from different channels are not correlated). Because phase of a complex number wraps to $-\pi$ and π , there is a phase wrapping problem. For example, simple numerical average of -0.9π and 0.9π gives 0. However, as shown in Fig. 2 (a), the correct phase “average” should be close to π , exactly the opposite to 0. By using the complex vector operation, rather than absolute phase numbers, Eq. (2) completely avoids this problem. In addition, the combined complex vector that is used to produce phase information in Eq. (2) corresponds to the least-squares solution of the multi-channel image combination problem, which gives high SNR in the phase reconstruction [17]. In essence, at a particular pixel, strong signals from some coils will suppress the noisy signals from the other channels, as shown in Fig. 2 (b).

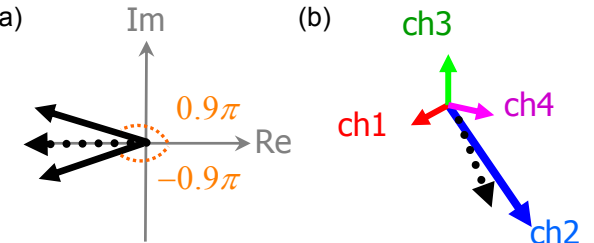


Figure 2. (a) Complex vector summation avoids phase wrapping in direct phase subtraction and average. (b) Weighted complex vector summation for high SNR reconstruction. The length of the vector represents the signal strength. The dashed arrow shows the optimally combined complex vector.

III. RESULTS

Data Acquisition

A sequence of in-vivo prostate data were acquired on a Signa HD 1.5T GE whole body clinical scanner (GE Healthcare, Waukesha, WI) using the commercially available 4-channel receivers connected to combined three torso surface coils and an endorectal coil during a contrast-enhanced study. An enhanced fast Gradient Echo 3-D pulse sequence was used with the parameters: TR / TE = 7 ms / 2.804 ms, receiver bandwidth = 41.67 kHz, FOV = 18 cm x 18 cm, image-matrix size = 256 x 256, total slice = 14, tip-angle = 15°, slice thickness = 3 cm, frequency / phase encoding step = 256 / 128, frames = 22, and scan-time = 9 min and 38 seconds. Figure 3 shows the magnitude and phase images from the four channels (the 5th frame and the

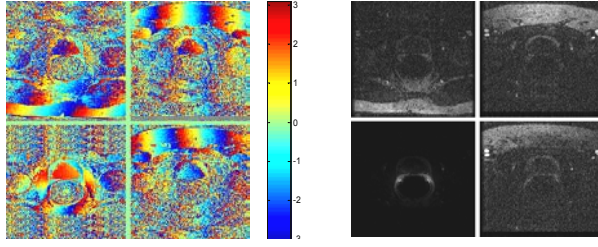


Figure 3. Representative phase (Left) and magnitude (Right) images from the 5-th frame and the 7-th slice of a 3D dynamic prostate MRI experiment.

middle slice). We used this data set to test the proposed algorithm, though no thermal ablation or flow was applied or measured in this experiment. Raw k-space data were transferred to a local Pentium 2.5 GHz computer for processing in MATLAB (The MathWorks, Natick, MA). The k-space data were retrospectively subsampled to simulate those would be acquired in accelerated scans.

Phase Image Reconstruction

The simulated subsampled data were reconstructed using the described auto-calibrating algorithm with block size = 2, column size = 3 and ACS = 32. FNF fitting scheme was used for model training. To obtain the phase-difference map, the first frame was used as the reference frame. After reconstruction, a phase difference map was generated using the proposed optimal phase combination algorithm.

For comparison, phase-sensitive SENSE imaging as in [3] was also performed using the same subsampled data. Using the low-resolution coil-sensitivity from the 32 ACS lines in the reference frame, a coil sensitivity map was created by dividing the coil images with the SOS image [9]. Then a complex image of the dynamic frame was obtained using SENSE, similarly as in [3,6]. A phase-difference map between the dynamic and the reference frames was obtained by taking the angle of the reconstructed complex image. In addition, zero-padded FFT reconstructions from the two central 32 central k-space lines were obtained. Low-resolution phase-difference maps were then computed by combining the 4-ch phase-difference maps using Eq. (2).

Performance Evaluation

To evaluate the phase reconstruction accuracy, a “ground truth” phase-difference map was established using the fully-encoded data frames, i.e., with all 128 phase encodings. In particular, high-resolution dynamic and reference complex images were reconstructed. The phase maps were then derived using the Eq. (2). Figure 4 compares the phase-difference maps from the three recon methods with the “ground truth”. As shown, MCMLI reconstructed phase-difference map is visibly more accurate and has higher SNR than the other two reconstructions. This is especially obvious around the edges of the structures.

To quantitatively examine the phase reconstruction accuracy,

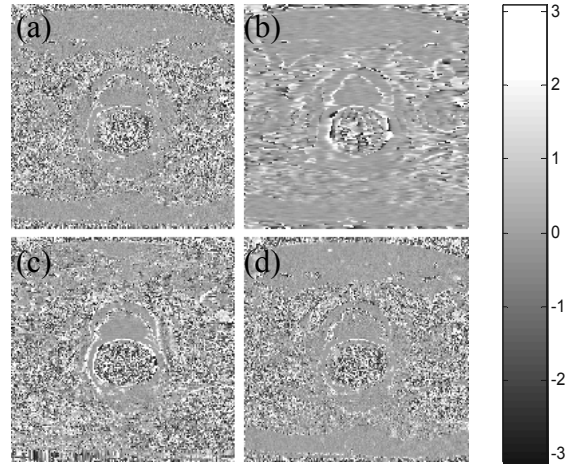


Figure 4. Phase-difference maps: (a) true phase-difference map using 128 encodings, (b) from zero-padded FFT recon with 32 encodings, (c) from SENSE recon with $R=2$, and (d) from the proposed method with $R=2$.

a region of interest (ROI) was manually selected to cover the prostate and rectum peripheral areas, as shown in Fig. 5. Histograms of phase errors associated with different reconstructions are generated in Fig. 5. The majority of phase errors in MCMLI reconstruction is distributed around zero, while SENSE and zero-pad FFT recons contain more pixels with larger errors over the range from $-\pi$ to π .

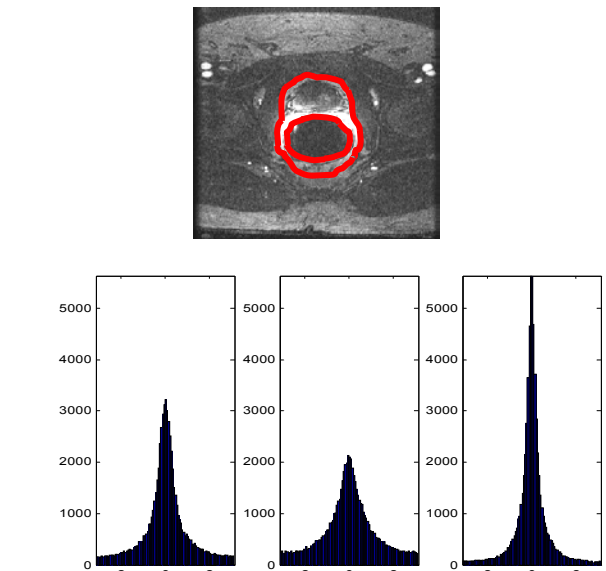


Figure 5. Histogram of phase error-map in the ROI (shown in red contour) for the reconstructions shown in Fig. 4: (Left) SENSE, (Middle) zero-pad FFT, (Right) the proposed method.

Figure 6 shows the phase map obtained by different channel phase combination methods. Clearly, the proposed optimal method has less phase errors. To see this quantitatively, mean angular error (MAE) metric is defined as

$$MAE = \sum_{(x,y) \in ROI} |\arg \{e^{j\Delta\theta_{recon}(x,y)} \cdot e^{-j\Delta\theta_{ground-truth}(x,y)}\}| / N \quad [3]$$

where N is the number of pixels in the ROI. The performance of three techniques was compared in Fig. 7 (a) and (b). As shown, in all frames and reduction factors examined, MCMLI achieved minimum MAE, showing over 50% less MAE as compared with SENSE and zero-padded FFT reconstruction techniques.

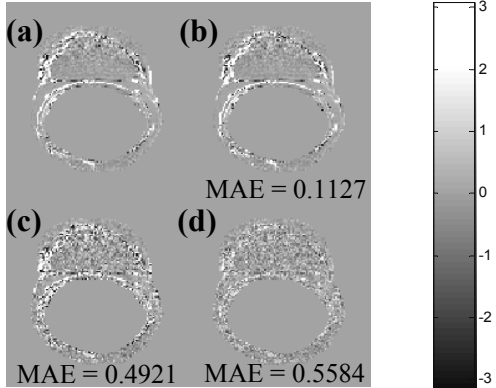


Figure 6. Phase maps of the ROI (as in Fig. 5) obtained by (a) “ground truth” from 128 encodings, and (b) from MCMLI recon with $R=2$ using the optimal combination method, (c) combination without optimal magnitude weighting, and (d) phase average. The optimal method gives best SNR in the prostate.

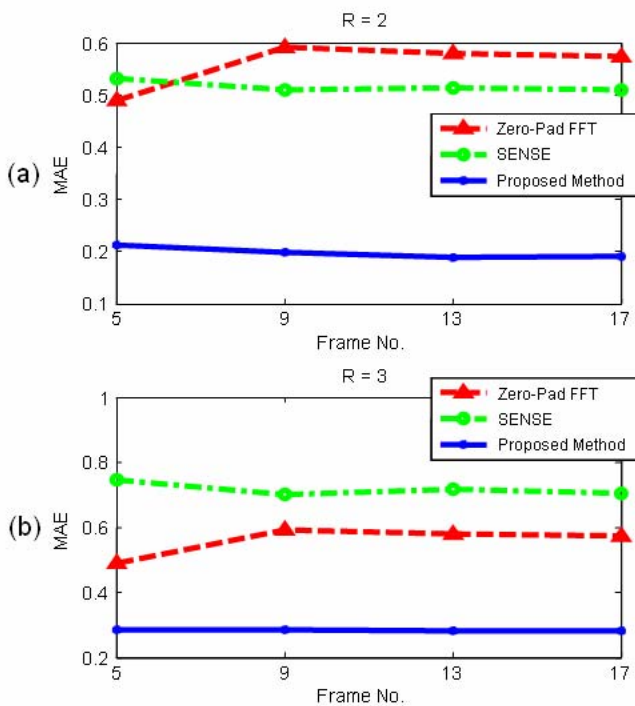


Figure 7. Phase reconstruction error of the three reconstruction methods for (a) $R = 2$ and (b) $R = 3$.

IV. DISCUSSIONS

Phase sensitive imaging was integrated with a self-calibrating k-space reconstruction method for parallel MRI. An optimal method was used to derive the dynamic phase

sensitive information from multiple phase-array images. Simulation results using 4-channel prostate imaging data demonstrated that the new method is more accurate than the SENSE method in recovering the phase information and it is robust against the image noises. The method has potentials to improve phase-sensitive MRI applications such as phase contrast velocity mapping, temperature mapping, and Dixon water/fat imaging.

ACKNOWLEDGEMENT

The authors thank Dr. Jingfei Ma from M. D. Anderson Cancer Center for providing the data used in the abstract.

REFERENCES

- [1] P. Thunberg, M. Karlsson, and L. Wigstrom, “Accuracy and Reproducibility in Phase Contrast Imaging Using SENSE,” *Magn. Reson. Med.*, vol. 50, pp. 1061-1068, 2003.
- [2] T. Kahn, T. Harth, J. Kiwit, H. Schwarzaier, C. Wald, and U. Modder, “In vivo MRI Thermometry Using a Phase-Sensitive Sequence: Preliminary Experience During MRI Guided Laser-Induced Interstitial Thermotherapy of Brain Tumors,” *J. of Magn. Reson.*, vol. 8, pp. 160-164, 1998.
- [3] J. A. Bankson, R. J. Stanfford, and J. D. Hazle, “Partially Parallel Imaging with Phase-Sensitive Data: Increased Temporal Resolution for Magnetic Resonance Temperature Imaging,” *Magn. Reson. Med.*, vol. 53, pp. 658-665, 2005.
- [4] P. Kellman, Y. Chung, E. R. McVeigh, and O. P. Simonetti, “SENSE Accelerated 3D Imaging of Myocardial Infarction using Phase Sensitive Inversion Recovery,” *Proc 11th Scientific Meeting ISMRM*, Toronto, pp. 1611, 2003.
- [5] W. Dixon, “Simple proton spectroscopic imaging,” *Radiology* 153:189-194, 1984.
- [6] J. S. van den Brink, Y. Watanabe, C. K. Kuhl, T. Chung, R. Muthupillai, M. V. Cauteren, K. Yamada, S. Dymarkowski, J. Bogaert, J. H. Maki, C. Matos, J. W. Casselman, and R. M. Hoogeveen, “Implications of SENSE MR in routine clinical practice,” *European J. Radiol.*, vol. 46, pp. 3-27, 2003.
- [7] J. Ma, J. B. Son, “A fast spin echo two-point Dixon technique and its combination with sensitivity encoding for efficient T2-weighted imaging,” *J. of Magn. Reson.*, vol. 23, pp. 977-982, 2005.
- [8] A. C. Brau, C. A. McKenzie, A. Shimakawa1, H. Yu, J. W. Johnson1, J. H. Brittain1, S. B. Reeder, “Accelerated IDEAL Water-Fat Separation Techniques for Single- and Multi-Coil Applications,” *Proc. Intl. Soc. Mag. Reson. Med.*, p. 491, 2005.
- [9] K. P. Pruessmann, M. B. Weiger, M. B. Scheidegger, and P. Boesiger, “SENSE: Sensitivity encoding for fast MRI,” *Magn. Reson. Med.*, vol. 42, pp. 952-962, 1999.
- [10] P. Thunberg, M. Karlsson, and L. Wigström, “Accuracy and reproducibility in phase contrast imaging using SENSE,” *Magn. Reson. Med.*, vol. 50, pp. 1061-1068, 2003.
- [11] P. M. Jakob, M. A. Griswold, R. R. Edelman, and D. K. Sodickson, “AUTO-SMASH: A self-calibrating technique for SMASH imaging,” *Magn. Reson. Med.*, vol. 13, pp. 42-54, 1998.
- [12] M. A. Griswold, P. M. Jakob, R. M. Heidemann, M. Nittka, V. Jellus, J. Wang, B. Kiefer, and A. Haase, “Generalized autocalibrating partially parallel acquisitions (GRAPPA),” *Magn. Reson. Med.*, vol. 47, pp. 1202-1210, 2002.
- [13] Z. Wang, J. Wang, and J. A. Detre, “Improved Data Reconstruction Method for GRAPPA,” *Magn. Reson. Med.*, vol. 54, pp. 738-742, 2005.
- [14] E. N. Yeh, C. A. McKenzie, M. A. Ohliger, and D. K. Sodickson, “3 Parallel Magnetic Resonance Imaging with Adaptive Radius in k-Space (PARS): Constrained Image Reconstruction using k-space Locality in Radiofrequency Coil Encoded Data,” *Magn. Reson. Med.*, vol. 53, pp. 1383-1392, 2005.
- [15] D. K. Sodickson, M. A. Griswold, and P. M. Jakob, “SMASH imaging,” *Magn. Reson. Imaging Clin. N. Am.*, vol. 7, pp. 237-54, 1999.
- [16] R. M. Heidemann, M. A. Griswold, A. Haase, and P. M. Jakob, “VD-AUTO-SMASH Imaging,” *Magn. Reson. Med.*, vol. 45, pp. 1066-1074, 2001.
- [17] M. A. Bernstein, M. Grgic, T. J. Brosnan and N. J. Pelc, “Reconstructions of Phase Contrast, Phased Array Multicoil Data,” *Magn. Reson. Med.*, vol. 32, pp. 330-334, 1994.